



HAL
open science

**Synthesis, antibacterial evaluation, crystal structure and
molecular interactions analysis of new
6-Bromo-2-chloro-3-butylquinazolin-4(3 H)-one**

Oussama Ouerghi, Mohammed Geesi, Abdellah Kaiba, El Hassane Anouar,
Abdul-Malek S. Al-Tamimi, Philippe Guionneau, Elmutasim O. Ibnouf,
Rachid Azzallou, Md Afroz Bakht, Yassine Riadi

► **To cite this version:**

Oussama Ouerghi, Mohammed Geesi, Abdellah Kaiba, El Hassane Anouar, Abdul-Malek S. Al-Tamimi, et al.. Synthesis, antibacterial evaluation, crystal structure and molecular interactions analysis of new 6-Bromo-2-chloro-3-butylquinazolin-4(3 H)-one. *Journal of Molecular Structure*, 2021, 1225, pp.129166. 10.1016/j.molstruc.2020.129166 . hal-02929647

HAL Id: hal-02929647

<https://hal.science/hal-02929647>

Submitted on 10 Sep 2020

HAL is a multi-disciplinary open access archive for the deposit and dissemination of scientific research documents, whether they are published or not. The documents may come from teaching and research institutions in France or abroad, or from public or private research centers.

L'archive ouverte pluridisciplinaire **HAL**, est destinée au dépôt et à la diffusion de documents scientifiques de niveau recherche, publiés ou non, émanant des établissements d'enseignement et de recherche français ou étrangers, des laboratoires publics ou privés.

Synthesis, Antibacterial Evaluation, Crystal Structure and Molecular Interactions Analysis of New 6-Bromo-2-chloro-3-butylquinazolin-4(3*H*)-one

Oussama ouerghi,^{1,5} Mohammed H. Geesi,² Abdellah Kaiba,¹ El Hassane Anouar,² Abdul-Malek S. Al-Tamimi,³ Philippe Guionneau,⁴ Elmutasim O.Ibnouf,^{6,7} Rachid Azzallou,⁸ Md Afroz Bakht,² Yassine Riadi,^{3*}

¹Department of physic, College of science and humanities in Al-Kharj, Prince Sattam bin Abdulaziz University, Al-Kharj 11942, Saudi Arabia

²Department of Chemistry, College of science and humanities in Al-Kharj, Prince Sattam bin Abdulaziz University, Al-Kharj 11942, Saudi Arabia

³Department of Pharmaceutical Chemistry, College of Pharmacy, Prince Sattam bin Abdulaziz University, Al-Kharj 11942, Saudi Arabia

⁴CNRS, Univ. Bordeaux, Bordeaux INP, ICMCB, UMR 5026, 87 av. Dr A. Schweitzer, F-33600 Pessac (France)

⁵Department of Pharmaceutics, College of Pharmacy, Prince Sattam bin Abdulaziz University, Al-Kharj 11942, Saudi Arabia

⁶Université Tunis El Manar, Tunis 1068, Tunisia

⁷Department of Medical Microbiology, Faculty of Medical Laboratory Sciences, Omdurman Islamic University, Sudan.

⁸Department of Process engineering and Environment, Faculty of Science and Technology Mohammedia, University of Hassan II -Casablanca, Morocco.

* Corresponding author. Tel.: +966 5 374 931 75; e-mail: y.riadi@psau.edu.sa/yassinriadi@yahoo.fr

Abstract

An efficient process was described to prepare a novel 6-bromo-2-chloro-3-butylquinazolin-4(3*H*)-one. The targeted compound was synthesized from available chemicals and was also assessed for anti-bacterial activity. This new compound structure crystalizes in the triclinic system with P-1 space group. Its unit cell parameters are ($a = 4.91550(10) \text{ \AA}$, $b = 11.4764(2) \text{ \AA}$, $c = 12.1670(3) \text{ \AA}$), volume ($638.11(4) \text{ \AA}^3$), $\alpha = 110.079(8)^\circ$, $\beta = 93.8130(10)^\circ$, $\gamma = 95.4580(10)^\circ$ and $Z = 2$. The crystal packing was stabilized by C=O...H hydrogen bonds and CH₃CH₂CH₂CH₂CHH...C π -stacking interaction and hydrogen π - π stacking interactions. Hirshfeld surfaces and their associated two-dimensional fingerprint plots were used to analyze the intermolecular interactions in the crystal structure. In addition, electrostatic surface potential (ESP) was generated using the density functional theory.

Keywords: 6-Bromo-2-chloro-3-butylquinazolin-4(3*H*)-one, Anti-bacterial, Crystal structure, Hirshfeld surface analysis.

1. Introduction

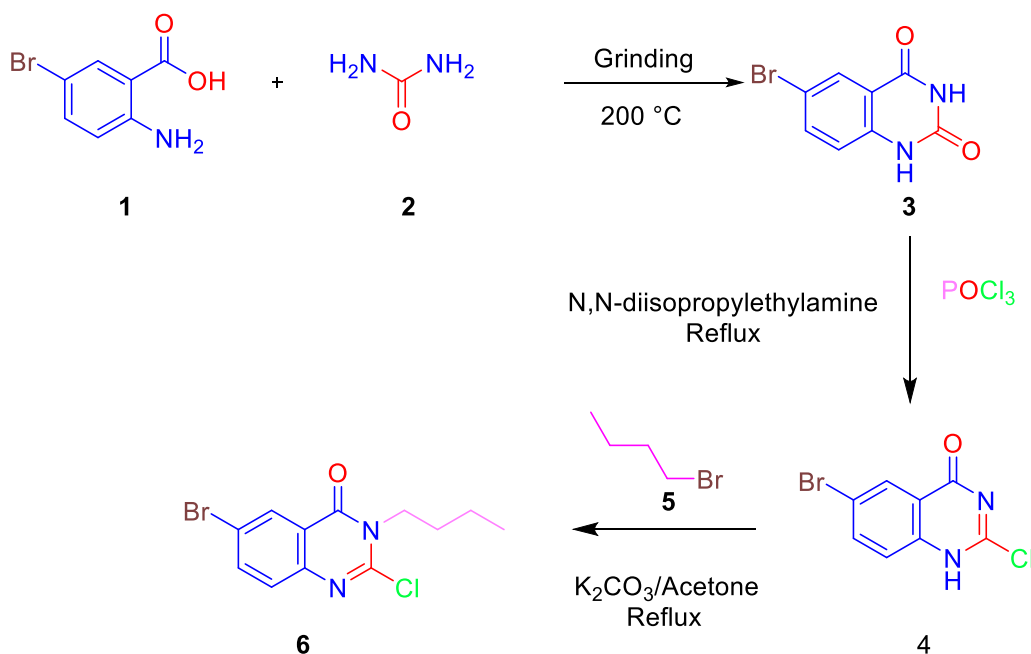
Quinazoline nuclei are diazotized heterocyclic compounds containing benzene and diazine cycles. These compounds are of great importance in the pharmacological and biological fields. Indeed, the quinazoline scaffold is present in the structure of many synthetic and natural compounds. The quinazoline derivatives show an important role in the preparation of versatile compounds that are biologically and pharmacologically active, such as: insecticides, herbicides [1], antifungals, [2] antibacterials, antivirals. [3] In fact, they are used as sedative agents [4], anthelmintics [5], potential radiosensitive agents [6], anti-tumor agents, [7-9] analgesic [10,11], anti-virus [12], anti-cytotoxin, anti-tuberculosis [13,14], antioxidant [15], antihypertension, anti-diabetes [16,17], etc. Pharmaceutical chemists prepared versatile types of quinazoline molecules that have shown variety of biological activities as efficient anti-allergic and anti-inflammatory drugs [18]. In addition, many examples of drugs were found such as proquazone [19], DQO-501 [20], and fluproquazone [21].

Therefore, and in continuation of on our research on the development of new routes to synthesize novel heterocyclic compounds [22-30]. Herein, we reported the preparation and the antibacterial activity assesment of novel quinazolinone molecule 6-bromo-2-chloro-3-butylquinazolin-4(3*H*)-one (**6**) with good yield (Scheme 1). Crystallographic investigations of the synthesized compound **6** were performed at room temperature, along with description of its molecular interactions, electrostatic surface potential (ESP) and fingerprint plots.

2. Synthesis

To prepare the targeted derivative, we used the procedure described in reference [31]. First, a mixture of urea (6 mmol) and 5-bromoanthranilic acid (1 mmol) was grinded in a mortar, then heated at 200 °C till total transfer of the mixture to liquid. This mixture was then cooled and NaOH solution (1N) was added, then the mixture was acidified using HCl solution (1N), until the total precipitation of intermediate **4**. The mixture was filtered to obtain the compound **4**. Then, compound **4** (17.6 mmol) was chlorinated in presence of phosphoryl chloride (176.4 mmol) and N,N-diisopropylethylamine (26.4 mmol) and the reaction was refluxed for 6 hours. Afterword, the reaction was cooled and the excess of phosphoryl chloride was removed *in vacuo*. Then, the resulting mixture was dissolved in dichloromethane DCM (25 mL) and washed using water and dried over magnesium sulfate. Finally, solvent removed by evaporation to obtain the 6-bromo-2-chloro-4(1*H*)-quinazolinone **4**. The intermediate **4** was reacted with an equimolar of 1-butylbromide (1 mmol) in acetone (10 mL) and in presence of anhydrous potassium acetate (1.5 mmol) and under continuous stirring overnight. Reaction progression was controlled by thin layer

chromatography [TLC]). The resulting solid was extracted using dichloromethane (3 X 10 mL), then the solvent was removed under vacuo and the obtained solid was purified through chromatography column (100 % DCM) to achieve the title derivative **6** as a yellow crystal (yield 81%).



Scheme 1. Strategy of the preparation of 6-bromo-2-chloro-3-Butylquinazolin-4(3H)-one (**6**)

1. Antibacterial activity

Synthesized molecule **6** was tested for the antibacterial activity against two gram-positive bacteria (Bacillus subtilis and methicillin resistant Staphylococcus aureus [MRSA]) and two gram-negative bacteria, (Escherichia coli and Pseudomonas aeruginosa) using a standard method documented in reference [32] and also described in detail in a previous article by our group [25].

Results of the antibacterial activity of the derivative **6** were cited in Table 1. This compound **6** showed good activity against two bacterial strains only.

Table 1. Activity of the derivative **6** against bacterial strains.

		Bacterial Strains			
		Pa	Ec	MRSA	Bs
Derivative 6	MIC (µg/ml)	- ^b	25	38.5	- ^b
	MBC (µg/ml)	- ^b	18.75	25	- ^b

	Inhibition zone in mm (100 µg/ml)	- ^b	20	16	- ^b
Ciprofloxacin	MIC (µg/ml)	12.5	12.5	18.75	12.5

^aMIC: Minimum inhibitory concentration in µg/mL. MBC: Minimum bactericidal concentration

^b: No inhibition zone, no activity.

3. Crystal structure

Crystal data and structure refinement details are summarized in Table 2. The collection data was carried out on Bruker Apex II diffractometer using a Molybdenum anticathode. A structural hypothesis was provided by SIR97 program [33]. The structure was solved by direct methods using SHELX97 program and all the atomic parameters are refined using a full-matrix least squares technique F^2 based on squared structure factor F^2 [34]. The non-hydrogen atoms were refined anisotropically but the hydrogen atoms were located theoretically. All the crystallography programs were used within the WINGX package [35]. The MERCURY program was used for Molecular graphics [36].

CCDC 2012234 contains crystallographic data for the present work. These data can be obtained free of charge via the following link: www.ccdc.cam.ac.uk/data_request/cif.

The structural resolution reveals that our compound crystallises in a triclinic system with a $P-1$ space group and unit parameters cell: $a = 4.91550(10) \text{ \AA}$, $b = 11.4764(2) \text{ \AA}$, $c = 12.1670(3) \text{ \AA}$, volume $(638.11(4) \text{ \AA}^3)$, $\alpha = 110.079(8)^\circ$, $\beta = 93.8130(10)^\circ$, $\gamma = 95.4580(10)^\circ$ and $Z = 2$. The molecular structure of the title compound is illustrated in **Figure 1**.

The Atomic positions (x, y, z) ($\times 10^4$) and equivalent isotropic displacement parameters U_{eq} ($\text{\AA}^2 \times 10^3$) are summarized in Table 3

Table 2: Crystallographic and structure refinement data

Empirical formula	C ₁₂ H ₁₂ Br Cl N ₂ O	
Formula weight	315.60	
Temperature	293(2) K	
Wavelength	0.71073 Å	
Crystal system	Triclinic	
Space group	P -1	
Unit cell dimensions	a = 4.91550(10) Å	α = 110.0790(10)°.
	b = 11.4764(2) Å	β = 93.8130(10)°.
	c = 12.1670(3) Å	γ = 95.4580(10)°.
Volume	638.11(2) Å ³	
Z	2	
Density (calculated)	1.643 Mg/m ³	
Absorption coefficient	3.415 mm ⁻¹	
F(000)	316	
Crystal size	0.160 x 0.080 x 0.080 mm ³	
Theta range for data collection	1.792 to 29.682°.	
Index ranges	-6 ≤ h ≤ 6, -15 ≤ k ≤ 15, -16 ≤ l ≤ 16	
Reflections collected	25187	
Independent reflections	3583 [R(int) = 0.0340]	
Completeness to theta = 25.242°	99.5 %	
Refinement method	Full-matrix least-squares on F ²	
Data / restraints / parameters	3583 / 0 / 155	
Goodness-of-fit on F ²	1.027	
Final R indices [I > 2σ(I)]	R ₁ = 0.0378, wR ₂ = 0.0984	
R indices (all data)	R ₁ = 0.0629, wR ₂ = 0.1106	
Largest diff. peak and hole	0.748 and -0.539 e Å ⁻³	

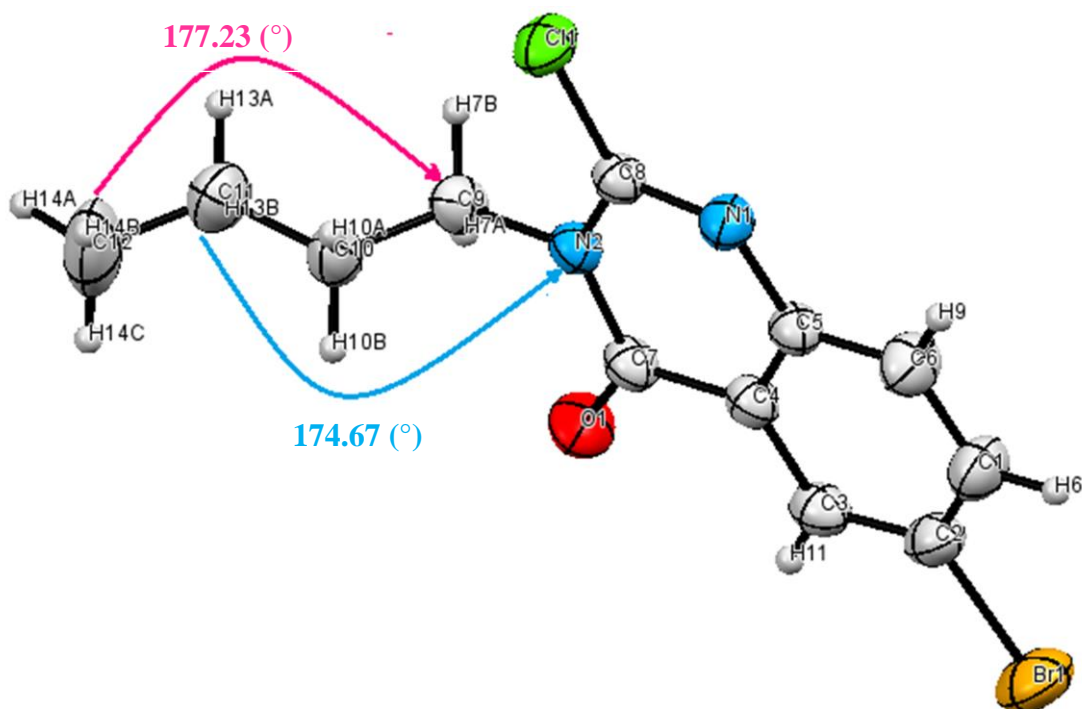


Figure 1: View along b axis of asymmetric unit cell of the titled compound.

x	y	z	U _{eq}
---	---	---	-----------------

Table 3:

Br(1)	7652(1)	9912(1)	8590(1)	65(1)
Cl(1)	-5656(1)	5642(1)	3540(1)	47(1)
O(1)	1954(4)	9061(2)	4284(2)	52(1)
C(4)	1740(5)	8174(2)	5768(2)	33(1)
C(8)	-2892(5)	6599(2)	4343(2)	32(1)
N(2)	-1595(4)	7544(2)	4036(2)	33(1)
C(2)	4740(5)	8808(2)	7543(2)	41(1)
N(1)	-1844(4)	6464(2)	5341(2)	37(1)
C(1)	3404(6)	7866(3)	7850(2)	48(1)
C(9)	-2663(5)	7740(2)	2955(2)	39(1)
C(5)	378(5)	7230(2)	6075(2)	34(1)
C(6)	1252(6)	7070(3)	7124(2)	45(1)
C(10)	-1519(6)	6951(3)	1864(2)	46(1)
C(3)	3971(5)	8957(2)	6496(2)	39(1)
C(7)	805(5)	8317(2)	4657(2)	36(1)
C(11)	-2881(7)	7100(3)	773(3)	57(1)
C(12)	-1758(10)	6394(5)	-330(3)	92(1)

Atomic
positions
($\times 10^4$) and
equivalent
isotropic

displacement parameter $U(\text{eq}) \text{ \AA}^2 \times 10^3$ for C₁₂ H₁₂ Br Cl N₂ O

The cohesion is ensured by hydrogen bonds, π stacking interaction and π - π stacking interaction between rings. The hydrogen bonds distances C=O...H and CH₃CH₂CH₂CHH...C π stacking

(**Figure. 2**) are respectively 2.390 Å and 2.878 Å. The π - π stacking interactions between rings of molecules are presented in **Figure. 3**, the centroid – centroid distances between two neighboring molecules is about 4.915 Å. The distance between carbon atoms C–C is between 1.368(4) and 1.516(4) Å. The C–N distance is between 1.350(3) Å and 1.481(3) Å. The C–Br distance is about 1.892(2) Å. and Å Finally, C=O distance is approximately 1.210(3) Å. The torsion angle value C12–C11–C10–C9 and C11–C10–C9–N2 is about 177.23 (°) and 174.77 (°) respectively, this shows that the CH₃–CH₂–CH₂–CH₂- is slightly twisted (Figure1).

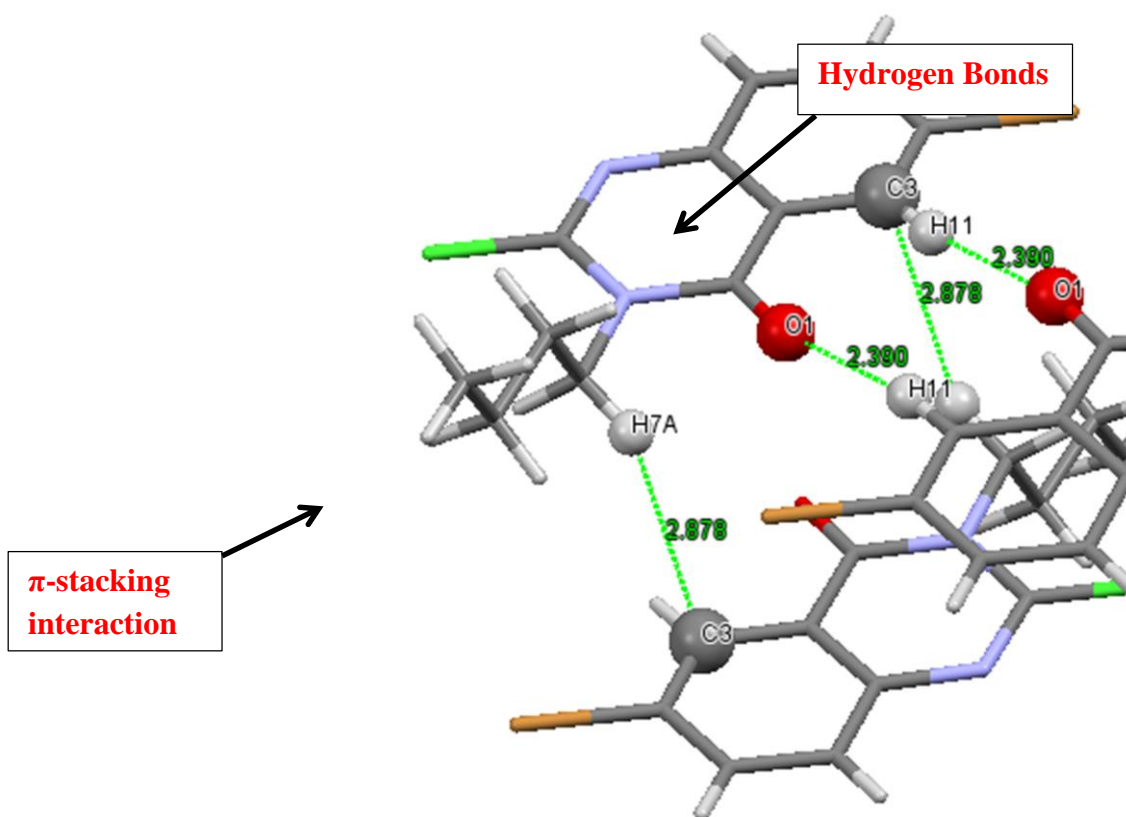


Figure 2: View showing the connection between the molecules by C=O...H hydrogen bonds and CH₃CH₂CH₂CHH...C π -stacking interaction (dashed lines).

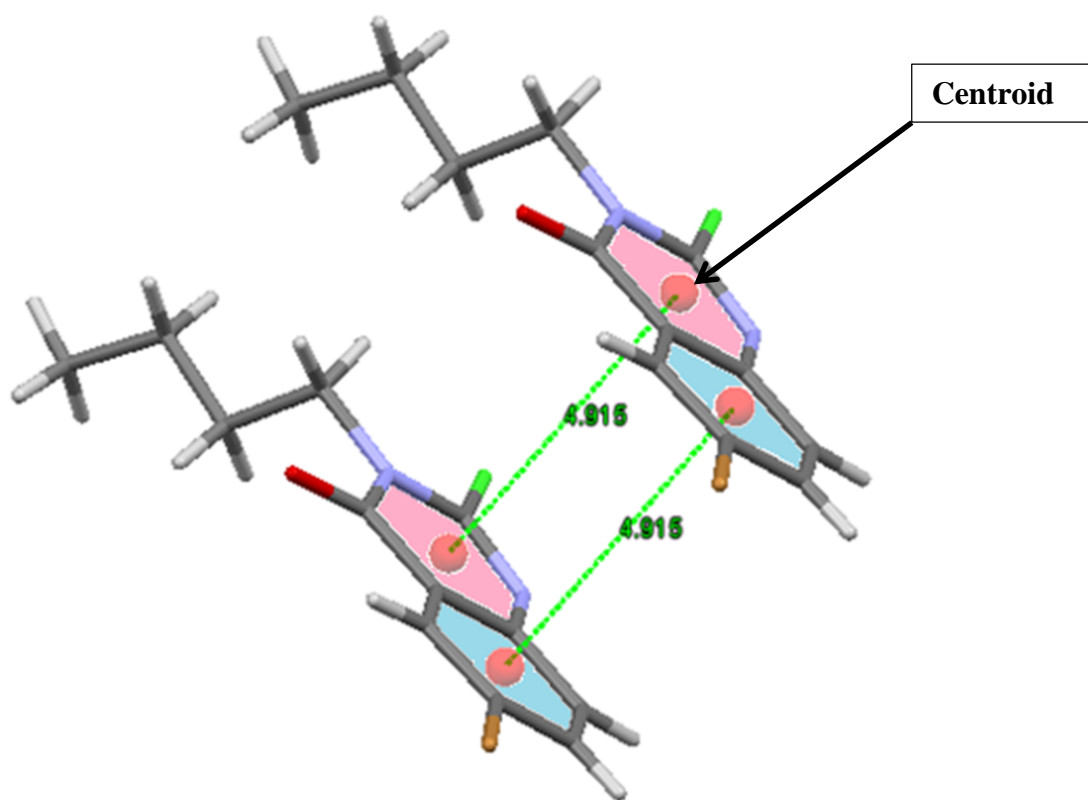


Figure 3: View showing the crystal cohesion by π - π stacking interactions between two neighboring molecules

The crystal structure is built via hydrogen bonds and π - π stacking interactions between neighboring molecules. These intermolecular interactions between molecules allows the crystal packing build up(**Figure 4**). Indeed, each molecule communicates with two other neighboring molecules through oxygen atom, butyl group and benzene via hydrogen bonds, π -stacking and trough π - π stacking interactions.

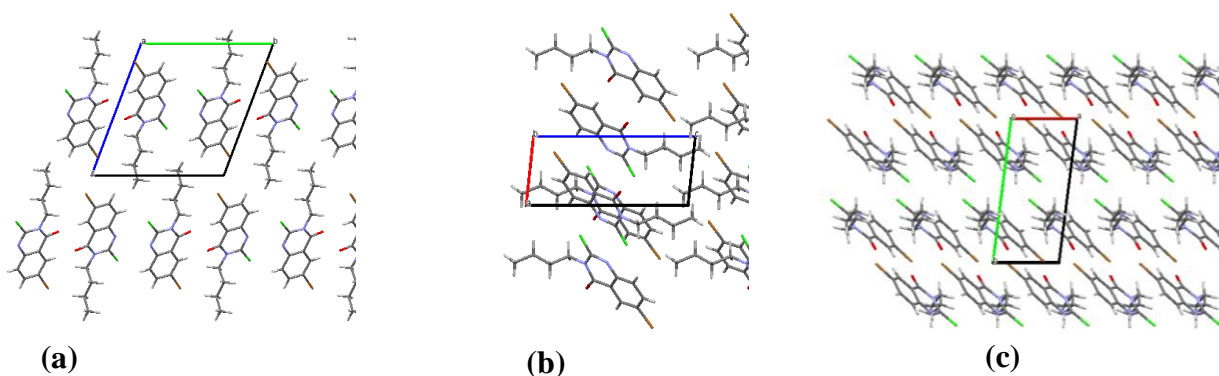


Figure 4: Packing of molecules in the crystal . a- Projection along a axis, b- Projection along b axis, c- Projection along c axis.

4. Computational details

4-1 Hirshfeld surface calculations

Hirshfeld surface and fingerprint plot of the $C_{12}H_{12}BrClN_2O$ were performed using Crystal Explorer 3.0 package [37]. The d_{norm} plots range delimited by -0.2759 a.u for blue color and 1.6303 a.u for red one. The red spots on the Hirshfeld surface indicate the interactions that involved intermolecular hydrogen bonding between $C_{12}H_{12}BrClN_2O$ units. 2D-fingerprint plots were displayed by using the expanded 0.6-2.8 Å. The electrostatic surface potential (ESP) of $C_{12}H_{12}BrClN_2O$ is determined at the DFT-B3LYP/6-311+G(d,p) level of theory using the Gaussian 16 package [38].

4-2 Hirshfeld surface analysis

Hirshfeld surface of $C_{12}H_{12}BrClN_2O$ mapped over the normalized contact distance d_{norm} is shown in Figure 5 (left). The red spots on the Hirshfeld surface indicate the formation of two strong hydrogen bonding of 2.241 Å between the units of $C_{12}H_{12}BrClN_2O$ (Figure 5, left). The first intermolecular hydrogen bond is established between the lone pair of the oxygen atom of the carbonyl group of quinazoline of the basic unit and the hydrogen atom of the aromatic ring at C5 position of the closest unit (Figure 5, left). The second hydrogen bond is formed between the hydrogen atom of the aromatic ring at C5 position of the basic unit and the lone pair of the oxygen atom of the carbonyl group of quinazoline of the closest unit (Figure 5, left). The Hirshfeld surface analysis reveals that the intermolecular interactions between are π -stacking interactions, and the units are stacked in head-to-tail one above the other. The intermolecular distance between the stacked units is of 3.84 Å (Figure 5, left).

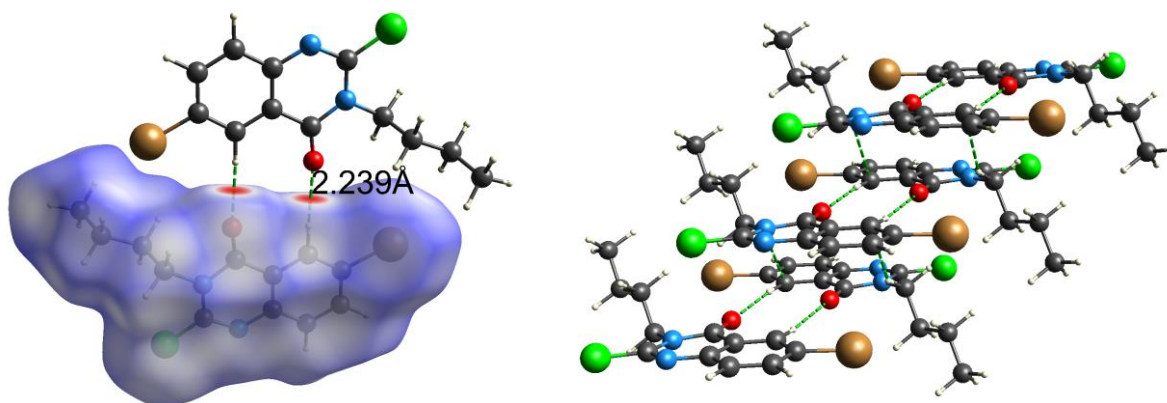


Figure 5: d_{norm} mapped on the Hirshfeld surface for visualizing intermolecular interactions of the title compound.

The electrostatic surface potentials (ESP) of $\text{C}_{12}\text{H}_{12}\text{BrClN}_2\text{O}$ is shown in Figure 6. In ESP, the red color is attributed to the negative region, which corresponds to hydrogen bond acceptors. However, the blue color indicates the positive region, which corresponds to hydrogen bond donors. As can be seen from Figure 6, the lone pair of oxygen atom of carbonyl moiety of quinazoline is a hydrogen bond acceptor. This result is in accordance with the Hirshfeld surface analysis, which show the formation of a strong intermolecular hydrogen bond between the one pair of oxygen atom of carbonyl moiety of quinazoline and the hydrogen atom of CH of the aromatic ring (**Figure 5**).

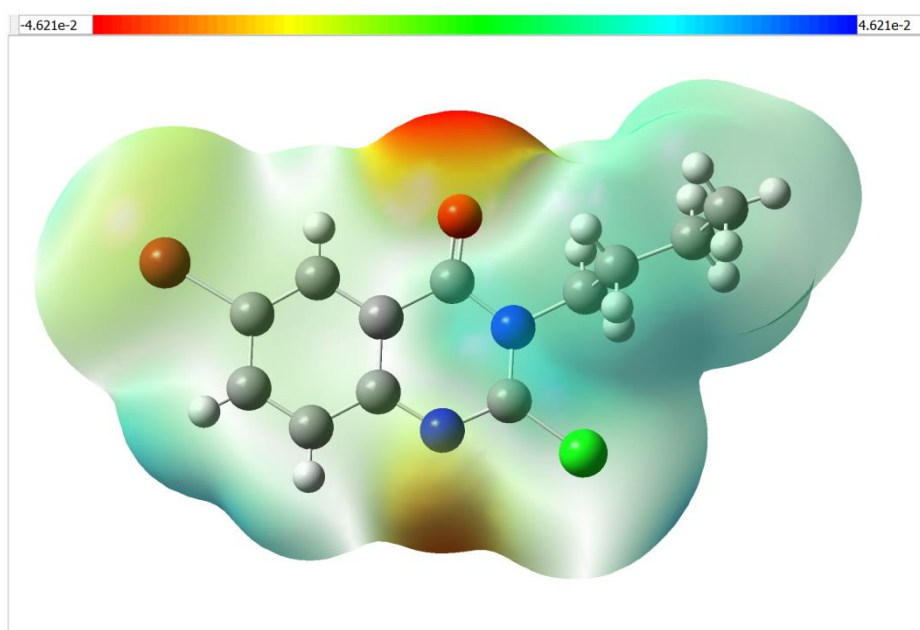


Figure 6: Electrostatic surface potential of $\text{C}_{12}\text{H}_{12}\text{BrClN}_2\text{O}$ obtained at the B3LYP/6-311+G(d,p) level of theory.

The 2D fingerprint plots for the most intercontacts between the $\text{C}_{12}\text{H}_{12}\text{BrClN}_2\text{O}$ units are shown in Figure 7 and the ratio of their contributions are summarized in Table 4. The highest inter atomic contact contribution were found between hydrogen atoms $\text{H}\cdots\text{H}$, about 39.6% (Figure 4), followed by $\text{Br}\cdots\text{H}/\text{H}\cdots\text{Br}$, $\text{Cl}\cdots\text{H}/\text{H}\cdots\text{Cl}$ and $\text{O}\cdots\text{H}/\text{H}\cdots\text{O}$ about 13.5, 8.0 and 7.4%, respectively.

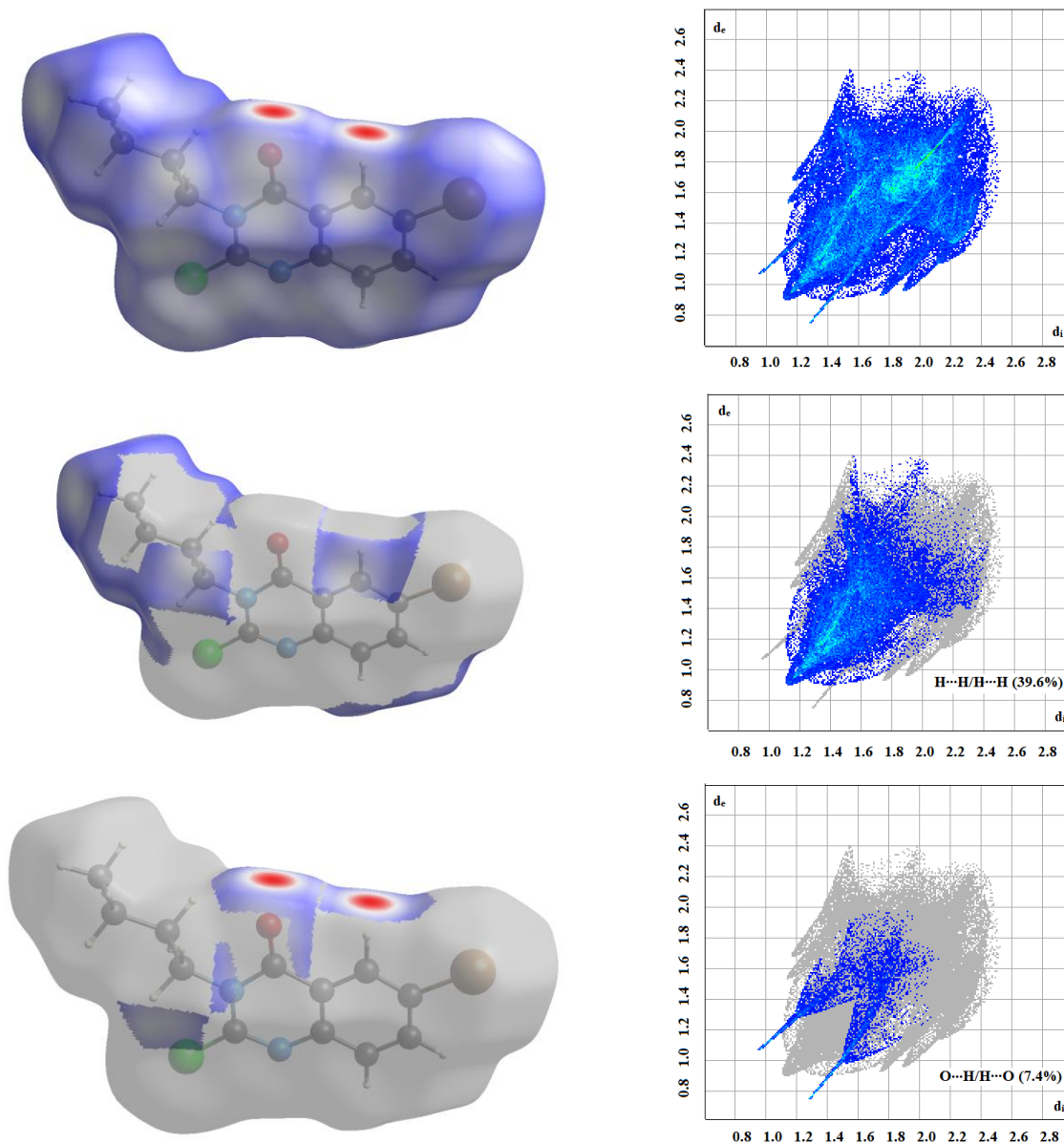


Figure 7: The two-dimensional fingerprint plots for the title compound showing all (up), $\text{Br}\cdots\text{H}/\text{H}\cdots\text{Br}$ (middle) and $\text{O}\cdots\text{H}/\text{H}\cdots\text{H}$ (bottom) closest intercontacts.

Table 4: Summary of the major closest contacts and their percentage contributions to the Hirshfeld surface.

Type of contact	Contribution (%)
$\text{H}\cdots\text{H}$	39.6
$\text{Br}\cdots\text{H}/\text{H}\cdots\text{Br}$	13.5
$\text{Cl}\cdots\text{H}/\text{H}\cdots\text{Cl}$	8.0

O··H/ H··O	7.4
C··H/ H··C	6

Conclusion

In summary, we have described the preparation of a new 6-bromo-2-chloro-3-butylquinazolin-4(3*H*)-one (**6**). Its anti - bacterial efficacy has been evaluated against different bacterial strains. The single crystal XRD structural studies of the 6-bromo-2-chloro-3-butylquinazolin-4(3*H*)-one was performed. The compound crystallized in monoclinic crystal system with P-1 space group. It exhibited hydrogen bond interaction C=O...H, CH₃CH₂CH₂CHH...C π -stacking interactions and slight π - π stacking interactions between rings of the molecule that assure the connection between molecules and stabilize the crystal. Moreover, the contribution of these interactions was also analysed by visualizing Hirshfeld surface. In addition, the electrostatic surface potential (ESP) was obtained using the DFT method.

Acknowledgments

The authors would like to thank the Deanship of Scientific Research at Prince Sattam Bin Abdulaziz University for providing financial support for this project (grant no. 2019/03/11064).

References:

- [1].S. Raw, C. Wilfred, R. Taylor, *J. K. Org, Biomol. Chem*, 2004, 2, 788.
- [2]. G. Cheeseman, R. Cookson, in: A. Weissberger, E.C. Taylor, *The Chemistry of Heterocyclic Compounds*, 35, John Wiley and Sons, New York, 1979, 1.
- [3].A. Porter, in: A. Katrizky, C. Rees, *Comprehensive Heterocyclic Chemistry*, 3, Pergamon Press, New York, 1984,195.
- [4]. Opitz, W., Jacobi, H., Pelster, B.: *Eur. Patent Ger. Offen. De.*, 220,438(Cl. C07D487/04), 01 Dec1983, Appl. 29 May 1982.
- [5].Pandey, M.P.: *Acta cien, Indica*, [Ser]. Chem., 1984, 10, 178.
- [6].Kalinowska, T.: *Acta Pol. Pharm.*, 1985, 42, 212.
- [7].Baguley, B.C.: DNA intercalating antitumor agents, *Anti-Cancer Drug Des.*, 1991, 6, 1- 35.
- [8].Brana, W.F., Castello, J.M., Keilhauter, G., Machuca, A., Martin, Y., Redondo,C., Schlick, E., Walker, N.: Benzimidazo[1,2-c]quinazolines: a new class of antitumor compounds, *Anti-Cancer Drug Des.* 1994, 9, 527-538.
- [9].Werbet, L.M., Angelo, M., Fry, D.W., Worth, D.F.: Basically substituted ellipticine analogues as potential antitumor agents, *J. Med. Chem*, 1986, 29, 1321-1322.
- [10]. Alagarsamy V, Solomon VR, Dhanabal K: Synthesis and pharmacological evaluation of some 3-phenyl-2-substituted-3H -quinazolin-4-one as analgesic, antiinflammatory agents. *Bioorg Med Chem* 2007, 15:235–241.
- [11]. Jataw V, Kashaw S, Mishra P: Synthesis and antimicrobial activity of some new 3-[5-(4-substituted)phenyl-1,3,4-oxadiazole-2yl]-2-styrylquinazoline-4(3H)-ones. *Med Chem Res* 2008, 17:205–211.
- [12]. Li H, Huang R, Qiu D, Yang Z, Liu X, Ma J, Ma Z: Synthesis and bioactivity of 4-quinazoline oxime ethers. *Prog Nat Sci* 1998, 8:359–365.

- [13]. Chandrika PM, Yakaiah T, Narsaiah B, Sridhar V, Venugopal G, Rao JV, Kumar KP, Murthy USN, Rao ARR: Synthesis leading to novel 2,4,6-trisubstitutedquinazoline derivatives, their antibacterial and cytotoxic activity against THP-1, HL-60 and A375 cell lines. *Indian J Chem* 2009, 48B:840–847.
- [14]. Nandy P, Vishalakshi MT, Bhat AR: Synthesis and antitubercular activity of Mannich bases of 2-methyl-3H-quinazolin-4-ones. *Indian J Heterocycl Chem* 2006, 15:293–294.
- [15]. Saravanan G, Alagarsamy V, Prakash CR: Synthesis and evaluation of antioxidant activities of novel quinazoline derivatives. *Int J Pharm Pharm Sci* 2010, 2:83–86.
- [16]. Hess HJ, Cronin TH, Scriabine A: Antihypertensive 2-amino-4(3H)-quinazolinones. *J Med Chem* 1968, 11:130–136.
- [17]. Malamas MS, Millen J: Quinazolineacetic acids and related analogs as aldosereductase inhibitors. *J Med Chem* 1991, 34:1492–1503.
- [18]. S. Johne, *Progress in Drug Research*, 26, 259-341 (1982).
- [19]. R. V. Coombs, R. P. Danna, M. Denzer, G. E. Hardtmann, B. Huegi, G. Koletar, J. Koletar, H. Ott, Jukniewicz, J. W. Perrine, E. J. Takesue and J. H. Trapold, *J Med. Chem.*, 16, 1237-45 (1973).
- [20]. M. Gilberto, S. D. Silva, C. M. R Sant'Anna and E. J Barreiro, *Bioorg. Med. Chem.*, 12, 3159-3166 (2004).
- [21]. J. W. Perrine, W. J. Houlihan and E. I. Takesue, *Arzneim. Forsch. / Drug Res.*, 34, 879-885 (1984).
- [22]. Y. Riadi, S. Massip, J.-M. Leger, C. Jarry, S. Lazar, and G. Guillaumet, 'Convenient synthesis of 2, 4-disubstituted pyrido [2, 3-d] pyrimidines via regioselective palladium-catalyzed reactions', *Tetrahedron*, vol. 68, no. 25, pp. 5018–5024, 2012.
- [23]. M. H. Geesi, M. E. Moustapha, M. A. Bakht, Y. Riadi, 'Ultrasound-accelerated green synthesis of new quinolin-2-thione derivatives and antimicrobial evaluation against Escherichia coli and Staphylococcus aureus', *Sustainable Chemistry and Pharmacy*, vol. 15, pp. 100195, 2020.
- [24]. Y. Riadi, 'UV Light Mediated Palladium-Catalyzed Synthesis of 2-Substituedpyrido[2,3-d]pyrimidines', *Polycyclic Aromatic Compounds*, pp. 1-6, 2019.
- [25]. M. H. Geesi, Y. Riadi, A. Kaiba, E. Anouar, O. Ouerghi, E. O. Ibnouf, P. Guionneaug, *Journal of Molecular Structure*, 1215, p. 128265, 2020.
- [26]. Y. Riadi, 'UV Light-mediated regioselective methylsulfanyl discrimination via Pd-catalyzed cross-coupling reactions of 2,4-dimethylsulfanylpyrido[2,3-d]pyrimidines', *Journal of Sulfur Chemistry*, vol. 40, no. 4, pp. 351-360, 2019.
- [27]. Y. Riadi, S. Lazar, G. Guillaumet, 'Regioselective palladium-catalyzed Suzuki–Miyaura coupling reaction of 2,4,6-trihalogenopyrido[2,3-d]pyrimidines', *Comptes Rendus Chimie*, vol. 22, no. 4, pp. 294-298, 2019.
- [28]. Y. Riadi, M. Geesi, O. Dehbi, M. A. Bakht, M. Alshammari, and M.-C. Viaud-Massuarde, 'Novel animal-bone-meal-supported palladium as a green and efficient catalyst for Suzuki coupling reaction in water, under sunlight', *Green Chemistry Letters and Reviews*, vol. 10, no. 2, pp. 101–106, 2017.

- [29]. Y. Riadi and M. Geesi, 'Photochemical route for the synthesis of novel 2-monosubstituted pyrido [2, 3-d] pyrimidines by palladium-catalyzed cross-coupling reactions', *Chemical Papers*, vol. 72, no. 3, pp. 697–701, 2018.
- [30]. M. H. Geesi, 'Synthesis, antibacterial evaluation, Crystal Structure and Hirshfeld surface analysis of a new 2-benzylsulfanyl-3-(4-fluoro-phenyl)-6-methyl-3H-quinazolin-4-one', *Journal of Molecular Structure*, p. 127894, 2020.
- [31]. T. Chihiro, O. Masataka, N. Hiromi, T. Yoshiji, Palladium(0)-Catalyzed Carbon-Hydrogen Bond Functionalization for the Synthesis of Indoloquinazolinones, *Advanced Synthesis & Catalysis*, 356(7), 1533-1538; 2014.
- [32]. E. H. Simpson, 'Prevalence of penicillin-resistant *Streptococcus pneumoniae*-Connecticut, 1992-1993, 1994.
- [33]. A. Altomare, M.C. Burla, M. Camalli, G.L. Cascarano, C. Giacovazzo, A. Guagliardi, A.G. Moliterni, G. Polidori, R. Spagna, SIR97: a new tool for crystal structure determination and refinement, *Journal of Applied Crystallography* 32(1) (1999) 115-119.
- [34]. G.M. Sheldrick, A short history of SHELX, *Acta Crystallographica Section A: Foundations of Crystallography* 64(1) (2008) 112-122.
- [35]. L.J. Farrugia, WinGX suite for small-molecule single-crystal crystallography, *Journal of Applied Crystallography* 32(4) (1999) 837-838.
- [36]. C.F. Macrae, I.J. Bruno, J.A. Chisholm, P.R. Edgington, P. McCabe, E. Pidcock, L. Rodriguez-Monge, R. Taylor, J. Streek, P.A. Wood, Mercury CSD 2.0—new features for the visualization and investigation of crystal structures, *Journal of Applied Crystallography* 41(2) (2008) 466-470.
- [37]. M. Turner, J. McKinnon, S. Wolff, D. Grimwood, P. Spackman, D. Jayatilaka, M. Spackman, *CrystalExplorer17*, University of Western Australia, 2017.
- [38]. M.J. Frisch, G.W. Trucks, H.B. Schlegel, G.E. Scuseria, M.A. Robb, J.R. Cheeseman, G. Scalmani, V. Barone, G.A. Petersson, H. Nakatsuji, X. Li, M. Caricato, A.V. Marenich, J. Bloino, B.G. Janesko, R. Gomperts, B. Mennucci, H.P. Hratchian, J.V. Ortiz, A.F. Izmaylov, J.L. Sonnenberg, Williams, F. Ding, F. Lipparini, F. Egidi, J. Goings, B. Peng, A. Petrone, T. Henderson, D. Ranasinghe, V.G. Zakrzewski, J. Gao, N. Rega, G. Zheng, W. Liang, M. Hada, M. Ehara, K. Toyota, R. Fukuda, J. Hasegawa, M. Ishida, T. Nakajima, Y. Honda, O. Kitao, H. Nakai, T. Vreven, K. Throssell, J.A. Montgomery Jr., J.E. Peralta, F. Ogliaro, M.J. Bearpark, J.J. Heyd, E.N. Brothers, K.N. Kudin, V.N. Staroverov, T.A. Keith, R. Kobayashi, J. Normand, K. Raghavachari, A.P. Rendell, J.C. Burant, S.S. Iyengar, J. Tomasi, M. Cossi, J.M. Millam, M. Klene, C. Adamo, R. Cammi, J.W. Ochterski, R.L. Martin, K. Morokuma, O. Farkas, J.B. Foresman, D.J. Fox, *Gaussian 16 Rev. C.01*, Wallingford, CT, 2016.